Journal of Alloys and Compounds 502 (2010) 112–117

Contents lists available at ScienceDirect

Journal of Alloys and Compounds

journal homepage: www.elsevier.com/locate/jallcom

Evaluation of the machinability of Ti–Sn alloys

Wen-Fu Ho[a], Shih-Ching Wu[b,c], Yu-Sheng Hong[d], Hsueh-Chuan Hsu[b,c,*]

[a] Department of Materials Science and Engineering, Da-Yeh University, Changhua, Taiwan, ROC
[b] Department of Dental Laboratory Technology, Central Taiwan University of Science and Technology, Taichung, Taiwan, ROC
[c] Institute of Biomedical Engineering and Material Science, Central Taiwan University of Science and Technology, Taichung, Taiwan, ROC
[d] Department of Mechanical and Automation Engineering, Da-Yeh University, Changhua, Taiwan, ROC

ARTICLE INFO

Article history:
Received 22 September 2009
Received in revised form 24 March 2010
Accepted 31 March 2010
Available online 7 April 2010

Keywords:
Metals and alloys
Mechanical properties
Scanning electron microscopy (SEM)

ABSTRACT

The machinability of a series of binary Ti–Sn alloys with Sn contents ranging from 1 to 30 mass% was investigated, using commercially pure titanium (c.p. Ti) as a control. The specimens were slotted using an electric dental handpiece and end mills. Machinability was evaluated by the cutting length, which traveled by the end mill from one edge of the specimen to the other edge. For each metal specimen, a permitted cutting time of 3 min was used to determine its average cut length. The experimental results indicated that alloying with Sn significantly improved the machinability of c.p. Ti in terms of cutting length under the present cutting conditions. The Ti–Sn alloys with a higher Sn concentration could be cut more readily. At 120 m/min, the lengths for Ti–20Sn were about 1.3 and 1.4 times higher than that of c.p. Ti at 200 and 300 gf, respectively. Additionally, the lengths for Ti–30Sn were about 1.7 and 1.8 times higher than that of c.p. Ti at 200 and 300 gf, respectively. For Ti–20Sn and Ti–30Sn, there was no adhesion of metal chips observed in the appearance of the cut surfaces at 120 m/min. Furthermore, they had the lowest surface roughness (Ra) values at 120 m/min. Our research suggests that the Ti–Sn alloys with Sn contents of 20 or 30 mass% developed here are viable candidates for machining at the rotation speed of 120 m/min by the CAD/CAM method.

1. Introduction

Cast pure titanium has been increasingly used to make fixed and removable prostheses. When compared with conventional dental alloys, it exhibits good biocompatibility, corrosion resistance and superior light weight [1–5]. However, the strength of titanium is inadequate for dental prostheses requiring comparatively high strength, such as partial dentures, bridges, and implants. Additionally, it is considered as one of the most difficult metals to machine (cut or grind) [6]. The poor machinability of titanium leads to a long processing time and short tool life [7,8]. Because of these inefficiencies, alloying titanium is one of the ways to improve its machinability properties.

The majority of the present dental alloys was developed with dental casting in mind. However, casting metals is not the only way to fabricate dental prostheses. The CAD/CAM (computer-aided design/computer-aided manufacture) method represents a great advancement over casting technology. Milling is the most important machining operation employed in many dental CAD/CAM systems [9,10]. Consequently, further development of new dental materials suited for machining is desired. This study, therefore, examined the machinability or the relative ease of machining these dental alloys. Over the past years, only a few studies have evaluated the machinability of dental alloys with the objective of developing new materials for dental CAD/CAM applications [11–14]. Machinability is defined as the relative ease of machining a metal. Kikuchi et al. [11–13] have examined the machinability of dental titanium alloys through the cutting force.

Among various titanium alloys, Ti–6Al–4V is one of the most studied, and has been used for the fabrication of denture bases and multiple unit bridges because its strength is superior to that of pure titanium [15]. In general, the grindability of Ti–6Al–4V is much better than that of pure titanium [16,17]. However, it has been speculated that the release of Al and V ions from the alloy might cause some long-term health problems [18–20]. For a metal to be used in a dental restoration, its biocompatibility is important so that it does not cause toxicological or allergic reactions. Therefore, caution should be exercised when alloying elements are added. In our previous research [21], a series of binary Ti–Sn alloys was developed which showed favorable mechanical properties. Tin (Sn) is known to be safe for use as an alloying element to titanium and is considered to be non-toxic and non-allergic [22]. Sn can also be used to strengthen Ti alloys [23]. In the present study, a new approach for evaluating machinability was applied to Ti–Sn alloys

* Corresponding author at: Department of Dental Laboratory Technology, Central Taiwan University of Science and Technology, No. 11, Buzih Lane, Beitun District, Taichung 40605, Taiwan, ROC. Tel.: +886 4 223 91647x7422.
E-mail addresses: hchsu@ctust.edu.tw, fujiiwfho@yahoo.com.tw (H.-C. Hsu).

0925-8388/$ – see front matter © 2010 Elsevier B.V. All rights reserved.
doi:10.1016/j.jallcom.2010.03.227

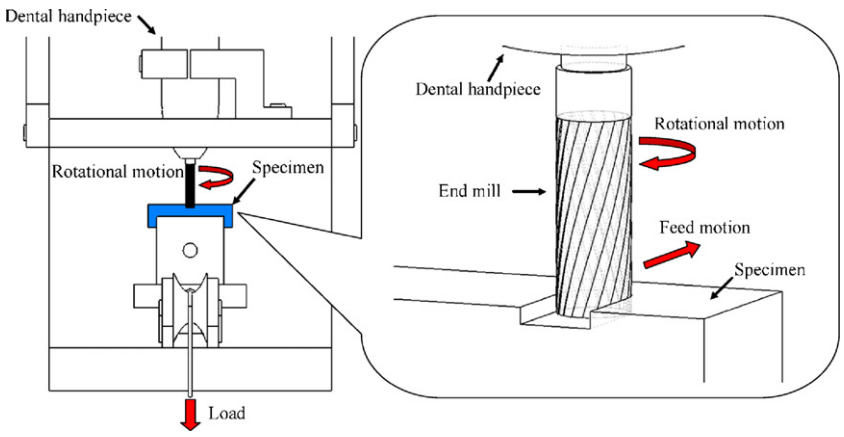

Fig. 1. Schematic illustration of the machinability test.

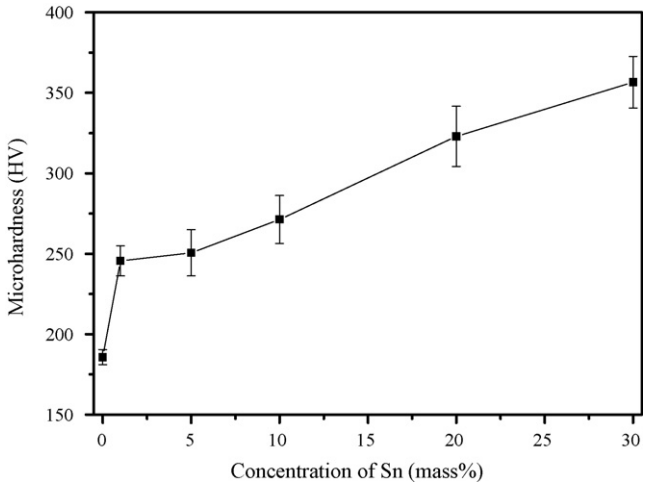

Fig. 2. Microhardness of c.p. Ti and Ti–Sn alloys.

up to 30 mass% Sn. This series of alloys was evaluated with the hope of developing a new titanium alloy suitable for dental CAD/CAM applications.

2. Materials and methods

The materials used in this study included commercially pure titanium (c.p. Ti) and a series of Ti–Sn alloys [1, 5, 10, 20 and 30 mass% Sn (hereafter, 'mass%' will be referred to as '%')]. All the materials were prepared from raw titanium (99.8% in purity), Sn (99.95% in purity) by using a commercial arc-melting vacuum-pressure-type casting system (Castmatic, Iwatani Corp., Japan). The melting chamber was first evacuated and purged with argon at a pressure of 1.5 kgf/cm^2 maintained during the melting process. Appropriate quantities of Ti and Sn were melted in a U-shaped copper hearth with a tungsten electrode. The ingots were re-melted five times prior to casting to improve their chemical homogeneity. Prior to casting, the ingots were again melted in an open-based copper hearth under an argon pressure of 1.5 kgf/cm^2. The difference in pressure between the two chambers allowed the molten alloys to instantly drop into the graphite mold when melted. The cast alloys were sectioned by using a Buehler Isomet low-speed diamond saw to obtain specimens. The microhardness of the polished alloys was measured by using a microhardness tester (MVK-E3, Mitutoyo, Japan) at 100 g for 15 s.

The specimens were slotted using an electric dental handpiece (Ultimate 500, NSK Nakanishi Inc., Japan) and end mills (DB-7, Dedeco International Inc., USA). A schematic diagram of the machinability test is illustrated in Fig. 1. Each specimen was fixed on a table that was moved by an applied load. A cutting test was performed under six cutting conditions, as shown in Table 1, for each specimen. By applying a force of 100, 200 or 300 gf, the specimens were milled at one of the two cutting speeds of the end mill (120 or 240 m/min). The cutting depth was 0.5 mm. Machinability was evaluated by the cutting length, which traveled by the end mill from one edge of the specimen for 3 min permitted calculation of the average cutting length for different metals. No cutting fluid or coolant was used. Three specimens were used to evaluate the machinability of each alloy and the test was performed twice

Table 1
Cutting conditions.

Condition	Rotation speed (m/min)	Load (gf)	Cutting depth (mm)
A	120	100	0.5
B	120	200	0.5
C	120	300	0.5
D	240	100	0.5
E	240	200	0.5
F	240	300	0.5

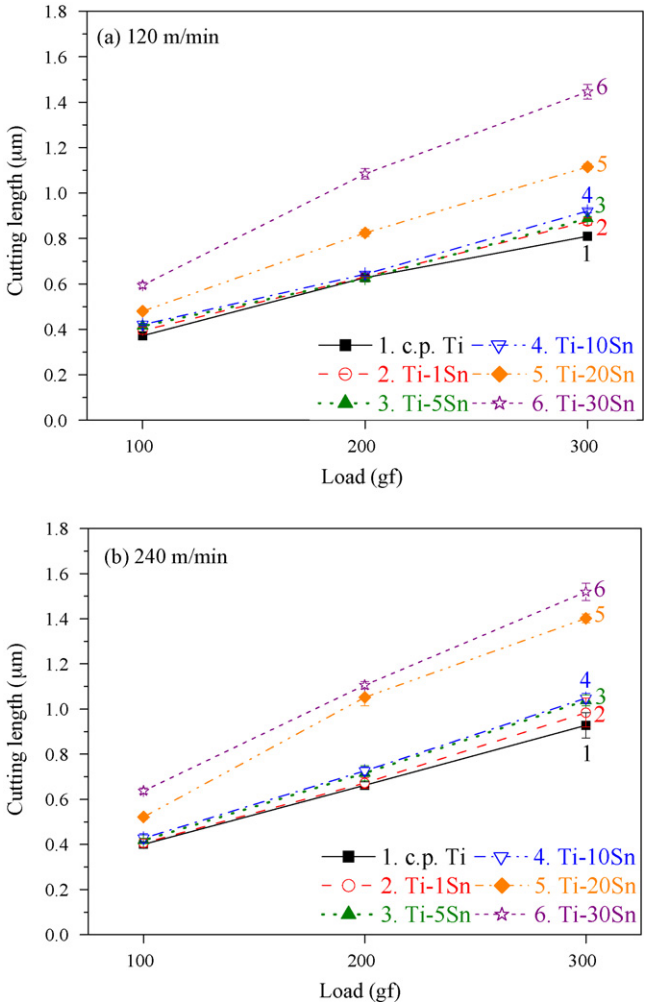

Fig. 3. Cutting length of c.p. Ti and Ti–Sn alloys.

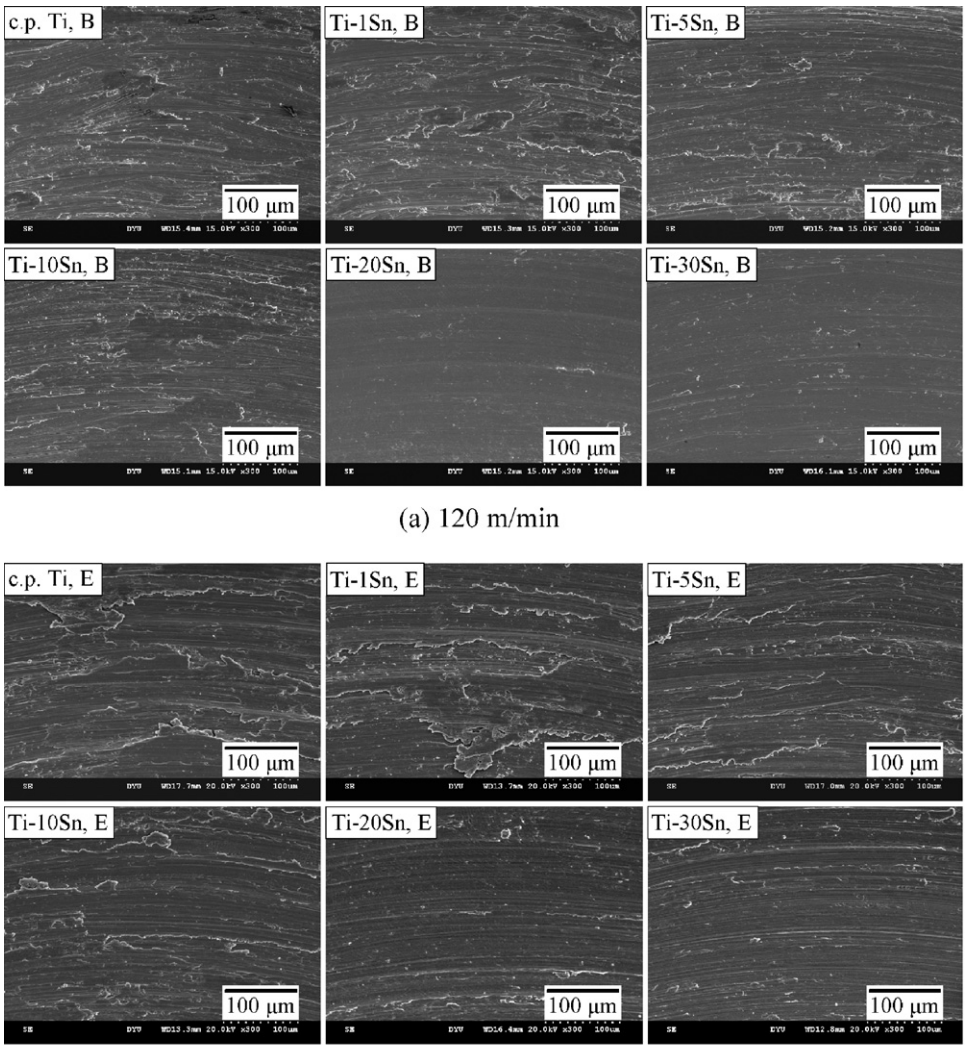

Fig. 4. Cut surfaces of c.p. Ti and Ti–Sn alloys.

for each kind of specimen at each cutting condition. All the surfaces subjected to cutting were abraded to the final level of a 2000-grit paper prior to testing.

After testing, the cut surfaces and metal chips were observed using a scanning electron microscope (SEM; S-3000N, Hitachi, Japan). The surface roughness (Ra) of the cut surfaces (bottom of the slots) was evaluated by using a surface texture measuring instrument (Surfcorder SE1700, Kosaka Corp., Japan).

3. Results and discussion

3.1. Microhardness

In our previous study [21], the phases of a series of Ti–Sn alloys were identified by using X-ray diffraction (XRD). The results indicated that the diffraction peaks of all the Ti–Sn alloys matched in α phase. There was no indication that β phase peaks or any intermediate phases were included in any of the diffraction patterns obtained. Fig. 2 shows the microhardness values of the c.p. Ti and Ti–Sn alloys. The hardness of the Ti–Sn alloys increased as the content of the Sn increased in a range between 246 HV (Ti–1Sn) and 357 HV (Ti–30Sn), and it was significantly higher ($p < 0.05$) than that of c.p. Ti (186 HV). Since the Ti–Sn alloys exhibited a complete solid solution (α phase) in the present study, their hardness values showed continuous change throughout the system. Of the Ti–Sn alloys, the alloy with 30% Sn content exhibited the highest hardness value, which was likely caused by the solid-solution hardening in the α phase. These results are similar to those obtained in the Ti–Zr alloy system reported by Ho et al. [24].

3.2. Machinability

The cutting lengths of the Ti–Sn alloys were determined for each load (100, 200 or 300 gf) at a rotation speed of 120 m/min and cutting depth of 0.5 mm, as shown in Fig. 3(a). The cutting lengths for Ti–20Sn and Ti–30Sn alloys were significantly higher ($p < 0.05$) than that for c.p. Ti. Up to 300 gf, the cutting lengths of all the Ti–Sn alloys and c.p. Ti tended to increase with the loads. The cutting lengths for the Ti–30Sn alloy were significantly higher ($p < 0.05$) than those of the other metals tested at any work loads. It is noteworthy that the lengths for Ti–30Sn were about 1.7 and 1.8 times higher than that of c.p. Ti at 200 and 300 gf, respectively. Additionally, the lengths for Ti–20Sn were about 1.3 and 1.4 times higher than that of c.p. Ti at 200 and 300 gf, respectively. On the other hand, the machinability of the Ti–Sn alloys with lower Sn concentrations (Sn ≤ 10%) was similar to that of c.p. Ti. There were no significant differences ($p > 0.05$) among the lengths for c.p. Ti, Ti–1Sn, Ti–5Sn and Ti–10Sn at the lower work loads of 100 and 200 gf.

The cutting lengths of the Ti–Sn alloys at a rotation speed of 240 m/min under three different loads (100, 200 or 300 gf) and

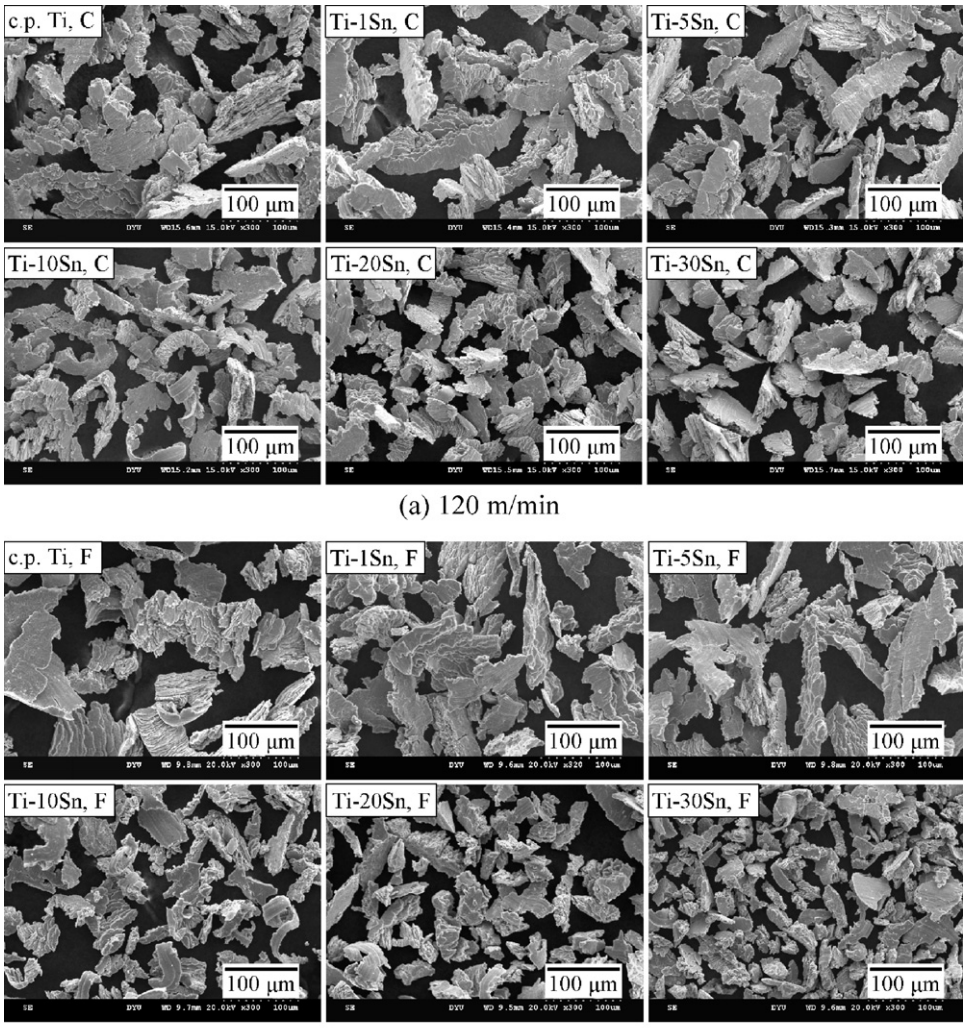

Fig. 5. Metal chips cut from c.p. Ti and Ti–Sn alloys.

cutting depth of 0.5 mm are shown in Fig. 3(b). Similar to the results at 120 m/min, the cutting lengths of all the Ti–Sn alloys and c.p. Ti tended to increase with the loads. The lengths for the Ti–20Sn and Ti–30Sn alloys were significantly higher ($p < 0.05$) than those of the other metals tested at any loads, especially at higher loads. At 200 gf, the lengths for Ti–20Sn and Ti–30Sn were about 1.6 and 1.7 times higher than that of c.p. Ti, respectively. At 300 gf, the lengths for Ti–20Sn and Ti–30Sn were about 1.5 and 1.6 times higher than that of c.p. Ti, respectively. It is noteworthy that, at 300 gf, the cutting lengths for the Ti–30Sn alloy were significantly higher ($p < 0.05$) than those of the Ti–20Sn alloy at 120 and 240 m/min.

The machinability of a metal is affected by its microstructure. Based on the Ti–Sn equilibrium phase diagram [25], the alloy phases of Ti–20Sn and Ti–30Sn alloys should be α phase and the intermetallic compound Ti_3Sn at room temperature. In general, the phases of as-cast alloys related closely to the cooling rate. If the cooling rate from the β-region is sufficiently rapid, martensitic structure α phase is formed, or the β phase is retained. Therefore, when using XRD to examine structural analysis, no peaks corresponding to intermetallic compound were detected in any of our specimens. Results similar to these can be found in our previous reports on Ti–Cr alloys [26]. As a result, the as-cast Ti–Sn alloys with Sn contents ranging from 1 to 30% consisted of α phases due to non-equilibrium cooling. Consequently, the machinability of the Ti–Sn alloys cannot be determined only by its microstructure.

It is known that lower ductility is generally beneficial to the machinability of metals [27,28]. In the steel industry, it is common to improve machinability by using sulfur [29] or various heat treatments [30] to decrease ductility. In our previous study [21], three-point bending tests were performed to evaluate the mechanical properties of Ti–Sn alloys. The results indicated that when the Sn content was 20% or greater, the alloys showed decreasing ductility. The Ti–20Sn alloy failed due to a combination of brittleness and ductility at an average deflection of about 6.3 mm, and Ti–30Sn failed entirely due to brittleness at an average deflection of only about 3.2 mm. In contrast, the other alloys (Ti–1Sn, Ti–5Sn and Ti–10Sn) did not fail, even after being deflected by 8 mm (the pre-set maximum). The ductility of Ti–Sn alloys became lower than that of c.p. Ti as the concentration of Sn increased [21]. In the present study, the cutting lengths (machinability) of the Ti–Sn alloys increased as the concentration of Sn increased. These results were similar to those found in other alloy systems by some researchers [12,13,31]. The magnitudes of cutting length for Ti–20Sn and Ti–30Sn were much higher than those for c.p. Ti and the other Ti–Sn alloys in the present study. The reduced ductility (lower bending deflection) was considered to be a primary contributing factor to the increased cutting lengths, as shown in Table 2.

Table 2
Bending deflections and cutting lengths of c.p. Ti and Ti–Sn alloys.

Alloy	Bending deflection (mm) [21]	Cutting length (mm)					
		A	B	C	D	E	F
c.p. Ti	>8.0	0.37	0.63	0.81	0.40	0.66	0.93
Ti–1Sn	>8.0	0.39	0.63	0.87	0.41	0.67	0.98
Ti–5Sn	>8.0	0.41	0.62	0.89	0.42	0.72	1.04
Ti–10Sn	>8.0	0.42	0.64	0.92	0.43	0.73	1.05
Ti–20Sn	6.3	0.48	0.82	1.12	0.52	1.05	1.40
Ti–30Sn	3.2	0.59	1.09	1.45	0.64	1.11	1.52

The fracture toughness (K_{IC}) values were computed from tensile properties on the basis of a fracture mechanics model that relates K_{IC} to tensile properties such as yield strength, tensile ductility and strain hardening exponent [28]. Chan et al. [28] indicated that fracture toughness increases with increasing ductility. Additionally, machinability increases with decreasing fracture toughness. Although the K_{IC} values of the cast Ti–Sn alloys intended for dental applications have not been measured in the present study. The greater cutting lengths of the Ti–20Sn and Ti–30Sn alloys are related to their lower ductility or lower K_{IC}.

Although many attempts have been made to explain and predict the machinability of a material by its strength or hardness, no general consensus has been reached regarding an explanation [12]. The hardness of the Ti–Sn alloys became higher than that of c.p. Ti as the contents of Sn increased. The increase in hardness was probably due to the solid-solution hardening of the α phase. Takeyama et al. [32] demonstrated that greater strength and hardness of a material generally render the machining thereof more difficult. However, in our study, the Ti–Sn alloys had greater hardness values than that of c.p. Ti, but they also had higher machinability, especially for Ti–20Sn and Ti–30Sn. In earlier studies [33–35], the respective researchers discussed grindability in terms of the hardness of the metals. Nevertheless, in the present study a high degree of hardness of a material does not necessarily result in low machinability. This result also agrees with that reported by Ohkubo et al. [16], who tested c.p. Ti and the Ti–6Al–4V alloy. In fact, it appears that hardness is not among the principal reasons for better machinability.

3.3. Observation of cut surfaces and metal chips

Fig. 4 shows the cut surfaces of the Ti–Sn alloys from rotation speeds of 120 and 240 m/min under a 200 gf load. The feed direction was from the bottom to the top, and the rotational direction was from the left to the right of each image. Cutting marks were observed on all the cut surfaces. However, cutting marks were observed to a greater degree for the c.p. Ti, Ti–1Sn, Ti–5Sn and Ti–10Sn alloys machined at 120 or 240 m/min. On the other hand, adhesion of metal chips to the cut surface was observed in some places for the c.p. Ti, Ti–1Sn, Ti–5Sn and Ti–10Sn alloys. Compared to 120 m/min, it was particularly obvious when the higher rotation speed (240 m/min) was employed. It is worth noting that there was no adhesion of metal chips in the appearance of the cut surfaces for Ti–20Sn and Ti–30Sn at 120 m/min.

Typical metal chips resulting from cutting at rotation speeds of 120 or 240 m/min and under a 300 gf load are illustrated in Fig. 5. For each metal, there were no pronounced differences in the appearance of metal chips among the c.p. Ti and Ti–Sn alloys. It should also be noted that in general, lower ductility promotes smaller chips. As shown in Fig. 6, the average size of the metal chips of Ti–Sn alloys decreased as the concentration of Sn increased between 52 and 62 μm at 120 m/min and between 34 and 61 μm at 240 m/min, and they were smaller than that of c.p.

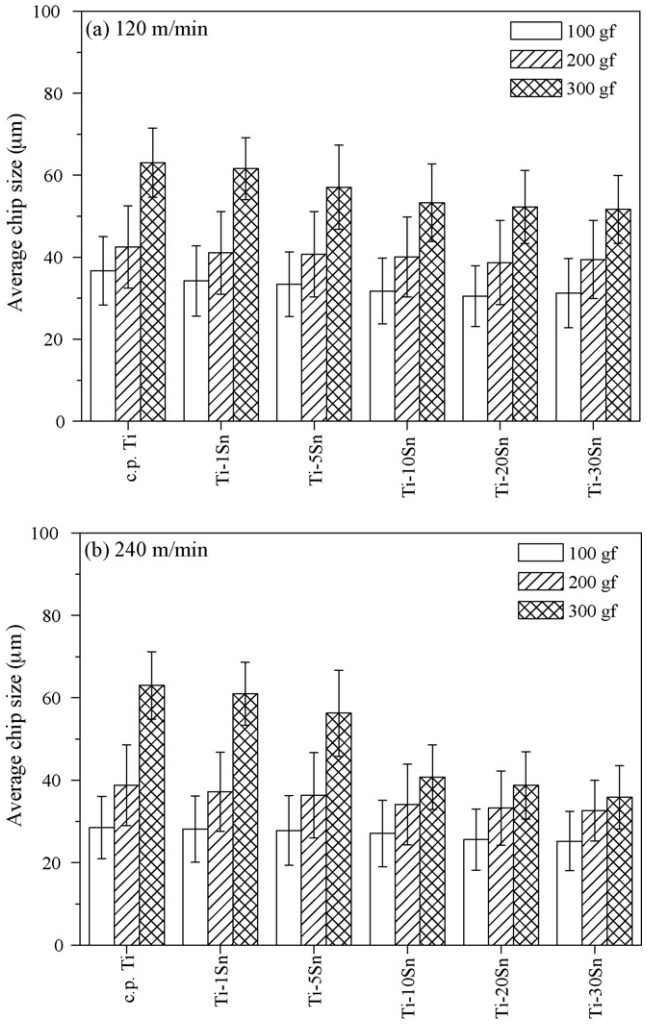

Fig. 6. Average size of metal chips of c.p. Ti and Ti–Sn alloys.

Ti (63 μm). Additionally, the chips appeared larger as the working load increased. From the viewpoint of chip control, the chips of all the metals were easily broken under the present condition. In the present study, it seems that finer metal chips are more suitable for machining than larger ones. This result was similar to those found in evaluating the grindability of Ti–Zr, Ti–Cr, Ti–Nb, Ti–Ag and Ti–Cu alloys [24,36–38]. Grindability is essentially the same process as cutting on a microscopic scale, and evaluating the grindability of a metal can be a guide to evaluating the ease of cutting [11].

3.4. Surface roughness

Fig. 7 shows the surface roughness values (Ra) of the cut surfaces of Ti–20Sn and Ti–30Sn in the feed directions at 120 and 240 m/min under the loads of 200 and 300 gf, respectively. It is evident that the specimens had better surface finish at 120 m/min when compared to a higher rotation speed of 240 m/min. Both Ti–20Sn and Ti–30Sn alloys had the lowest Ra values at the rotation speed of 120 m/min. The Ra values were increased when rotation speed was increased to 240 m/min for both alloys. The Ra values obtained at 120 m/min was about 1.1 μm, while at 240 m/min the range was between 1.4 and 1.7 μm. Results also showed that work loads do not seem to affect the surface finish of the metals under the same rotation speeds.

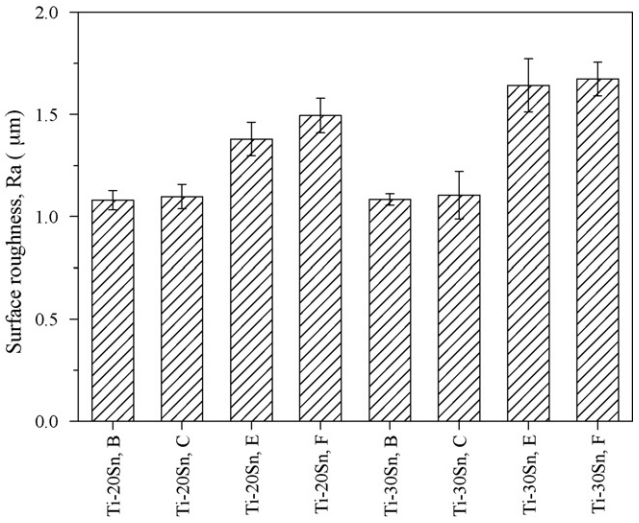

Fig. 7. Surface roughness values (Ra) of cut surfaces of Ti–20Sn and Ti–30Sn.

4. Conclusions

(1) The cutting lengths (machinability) of the Ti–Sn alloys increased as the concentration of Sn increased. Furthermore, the lengths of all the Ti–Sn alloys and c.p. Ti tended to increase with the loads. At 120 m/min, the lengths for Ti–20Sn were about 1.3 and 1.4 times higher than that of c.p. Ti at 200 and 300 gf, respectively. Additionally, the lengths for Ti–30Sn were about 1.7 and 1.8 times higher than that of c.p. Ti at 200 and 300 gf, respectively.

(2) At 240 m/min, the lengths for Ti–20Sn and Ti–30Sn were about 1.6 and 1.7 times higher than that of c.p. Ti at 200 gf, respectively. Moreover, the lengths for Ti–20Sn and Ti–30Sn were about 1.5 and 1.6 times higher than that of c.p. Ti at 300 gf, respectively.

(3) The adhesion of metal chips to the cut surface was observed in some places for the c.p. Ti, Ti–1Sn, Ti–5Sn and Ti–10Sn alloys. However, there was no adhesion of metal chips in the appearance of the cut surfaces for Ti–20Sn and Ti–30Sn at 120 m/min.

(4) Under the load of 300 gf, the average size of the metal chips of Ti–Sn alloys decreased as the concentration of Sn increased between 52 and 62 μm at 120 m/min and between 34 and 61 μm at 240 m/min, and they were smaller than that of c.p. Ti (63 μm).

(5) Both Ti–20Sn and Ti–30Sn alloys had the lowest surface roughness (Ra) values, about 1.1 μm, at the rotation speed of 120 m/min.

Acknowledgement

The authors acknowledge the partial financial support of National Science Council of Taiwan (NSC 97-2221-E-212-009 and NSC 98-2221-E-212-013).

References

[1] E.P. Lautenschlager, P. Monaghan, Int. Dent. J. 43 (1993) 245–253.
[2] M. Yamauchi, M. Sakai, J. Kawano, Dent. Mater. 7 (1988) 39–47.
[3] B. Bergman, C. Bessing, G. Ericson, P. Lundquist, H. Nilson, M. Andersson, Acta Odontol. Scand. 48 (1990) 113–117.
[4] M. Kononen, J. Rintanen, A. Waltimo, P. Kempainen, J. Prosthet. Dent. 73 (1995) 4–7.
[5] J.E. Rubenstein, J. Prosthet. Dent. 74 (1995) 284–293.
[6] O. Ozugwu, M. Wang, J. Mater. Process. Technol. 68 (1997) 262–274.
[7] J.F. Kahles, M. Field, D. Eylon, F.H. Froes, J. Metals 37 (1985) 27–35.
[8] T. Miyazaki, Y. Tamaki, E. Suzuki, T. Miyaji, J. Jpn. Dent. Mater. 6 (1987) 917–922.
[9] D. Rekow, J. Prosthet. Dent. 58 (1987) 512–516.
[10] C. Zimmerman, S.P. Boppana, K. Katbi, in: J.R. Davis (Ed.), Metals Handbook: Machining, vol. 16, ninth ed., ASM International, Materials Park, OH, 1989, pp. 639–647.
[11] M. Kikuchi, O. Okuno, Dent. Mater. J. 23 (2004) 37–45.
[12] M. Kikuchi, M. Takahashi, O. Okuno, Mater. Trans. 49 (2008) 800–804.
[13] M. Kikuchi, M. Takahashi, O. Okuno, Dent. Mater. J. 27 (2008) 216–220.
[14] M. Kikuchi, Acta Biomater. 5 (2009) 770–775.
[15] N. Wakabayashi, M. Ai, J. Prosthet. Dent. 77 (1997) 583–587.
[16] C. Ohkubo, I. Watanabe, J.P. Ford, H. Nakajima, T. Hosoi, T. Okabe, Biomaterials 21 (2000) 421–428.
[17] I. Watanabe, S. Kiyosue, C. Ohkubo, T. Aoki, T. Okabe, J. Biomed. Mater. Res. 63 (2002) 760–764.
[18] P.R. Walker, J. LeBlanc, M. Sikorska, Biochemistry 28 (1989) 3911–3915.
[19] S. Yumoto, H. Ohashi, H. Nagai, S. Kakimi, Y. Ogawa, Y. Iwata, K. Ishii, Int. J. PIXE 2 (1992) 493–504.
[20] S. Rao, T. Ushida, T. Tateishi, Y. Okazaki, S. Asao, Biomed. Mater. Eng. 6 (1996) 79–86.
[21] H.C. Hsu, S.C. Wu, Y.S. Hong, W.F. Ho, J. Alloys Compd. 479 (2009) 390–394.
[22] M. Niinomi, Sci. Technol. Adv. Mater. 4 (2003) 445–454.
[23] M. Niinomi, Metall. Mater. Trans. 33A (2002) 477–486.
[24] W.F. Ho, W.K. Chen, S.C. Wu, H.C. Hsu, Mater. Sci. Mater. Med. 19 (2008) 3179–3186.
[25] J.L. Murray, in: J.L. Murray (Ed.), Phase Diagrams of Binary Titanium Alloys, ASM International, Materials Park, OH, 1987, p. 294.
[26] W.F. Ho, T.Y. Chiang, S.C. Wu, H.C. Hsu, J. Alloys Compd. 468 (2009) 533–538.
[27] T. Okabe, M. Kikuchi, C. Ohkubo, M. Koike, O. Okuno, Y. Oda, J. Miner. Met. Mater. Soc. 56 (2004) 46–48.
[28] K.S. Chan, M. Koike, T. Okabe, Metall. Mater. Trans. 37A (2006) 1323–1331.
[29] J. Bellot, Met. Sci. Heat Treat. 22 (1980) 794–799.
[30] A.G. Guy, Physical Metallurgy for Engineers, Addison-Wesley, MA, 1962.
[31] M. Takahashi, M. Kikuchi, O. Okuno, Mater. Trans. 50 (2009) 859–863.
[32] H. Takeyama, T. Yoshikawa, T. Takada, J. Jpn. Soc. Preci. Eng. 41 (1975) 392–394.
[33] R. Grajower, I. Kurz, M.S. Bapna, Dent. Mater. 2 (1986) 187–192.
[34] M.H. Reisbick, R.F. Bunshah, J. Dent. Res. 52 (1973) 1138–1146.
[35] W.J. O'Brien, Dental Materials: Properties and Selection, Quintessence, Chicago, 1989.
[36] H.C. Hsu, S.C. Wu, J.Y. Chiang, W.F. Ho, J. Alloys Compd. 476 (2009) 817–825.
[37] M. Kikuchi, M. Takahashi, O. Okuno, Dent. Mater. J. 22 (2003) 328–342.
[38] M. Kikuchi, M. Takahashi, T. Okabe, O. Okuno, Dent. Mater. J. 22 (2003) 191–205.